



Thermal mechanical constitutive model of fiber reinforced shape memory polymer composite: Based on bridging model



Qiao Tan^a, Liwu Liu^b, Yanju Liu^b, Jinsong Leng^{a,*}

^a Centre for Composite Materials and Structures, Harbin Institute of Technology (HIT), No. 2 YiKuang Street, PO Box 3011, Harbin 150080, People's Republic of China

^b Department of Astronautical Science and Mechanics, Harbin Institute of Technology (HIT), P.O. Box 301, No. 92 West Dazhi Street, Harbin 150001, People's Republic of China

ARTICLE INFO

Article history:

Received 7 January 2014

Received in revised form 3 May 2014

Accepted 6 May 2014

Available online 16 May 2014

Keywords:

A. Polymer-matrix composites (PMCs)

B. Thermomechanical

C. Computational modeling

ABSTRACT

The ever increasing applications of Shape Memory Polymers (SMPs) and its Composites (SMPCs) have motivated the development of appropriate constitutive models. In this work, based on composite bridging model, a constitutive model for unidirectional SMPCs under thermal mechanical loadings in the small strain range has been developed. The composite bridging model has been adopted to describe the distribution of stress–strain between fiber reinforcement and SMPs matrix. Besides, considering the influence of fiber content and temperature, the storage and release of “frozen strain”, the recovery of stress has been quantified as well. The stress–strain curves of SMPCs laminate under axial tensile indicate that the theoretical data derived from the developed model are basically accordant with the experimental data, and that the proposed model is suitable for machining practice. Furthermore, the model has been applied to predict stress recovery, strain storage and releasing with changing of temperature.

© 2014 Elsevier Ltd. All rights reserved.

1. Introduction

Shape Memory Polymer and its Composites (SMPCs) are a class of smart materials that have the ability to return from a deformed state to their original shape at an external stimulus, such as heat, light, electricity and so forth [1–12]. SMPCs consist of a ‘stiff’ reinforcement and a ‘softer’ matrix arranged together with one phase distributed as an array inside of the other phase. The best known example of this type of composite is fibrous composite, where the ‘stiff phase’ is usually long thin fibers, graphite, glass or boron [13,14]. This type of composite owns many outstanding mechanical properties, such as high stiffness, strength and thermo-elastic stability, good corrosion resistance and thermal insulation [15–20]. Besides, for the stiffness and the strength of the carbon fiber are much higher than SMP matrix, the obtained composite generates a higher value of stress during process of the deformation recovery, and this is a desirable feature in engineering applications.

Because of these advantages, SMPCs are widespread in many branches of engineering within areas of applications ranging from biomedical devices, aircrafts, ships, and space vehicles to bridges, buildings, and storage vessels [21,22]. Designing of SMPCs based devices involves the need for strain–stress prediction to achieve

a satisfactory performance under the required conditions [23]. Thus it is necessary to develop appropriate constitutive models that can be used as simulation tools to assist the designs of SMPCs based structures.

A number of researchers have described the thermo-mechanical behavior of the SMPs and its composites [24,25]. The modeling efforts have split into several directions. In one direction, the shape memory effect is attributed to the formation of phases during cooling which serves to lock the temporary shape and a loss of the phases due to heating when shape recovery occurs. Models based on this concept include the 1D model by Liu et al., 3D models by Barot et al. for semicrystalline SMPs, Qi et al. and Chen and Lagoudas for general SMPs [26–35]. Besides, some earlier modeling efforts have adopted rheological models consisting of spring, dashpot, and frictional elements in constitutive models [36]. Description of micro-scale features, such as cross-linking, chain mobility, interface motion and entanglement of polymer molecules, is the third direction of SMPs modeling approaches, which including recent models by Nguyen et al., Castro et al. and so forth [37,38].

Although these models have improved the understanding of SMPs and its composites, more complicated models are needed to predict the thermo-mechanical characteristic of fiber reinforced SMPCs. However, a little research about the constitutive relationship of unidirectional fiber reinforced SMPCs have been done. In this study, based on composite bridging model theory and the continuum thermodynamic considerations, a 3D constitutive model

* Corresponding author. Tel./fax: +86 451 86402328.

E-mail address: lengjs@hit.edu.cn (J. Leng).

has been developed to simulate the stress–strain–temperature relationship of unidirectional elastic carbon fiber reinforced SMPCs [39,40]. To capture the thermo-mechanical response of this family of composites, we assume the material as a mixture of elastic reinforcement and SMP matrix, which is further divided into a continuum mixture of a glassy and a rubbery phase, and the fraction of each phase is complementary variation depending on the temperature. Using the theory of composite bridging model, we then incorporate the influence of elastic fiber reinforcement in the constitutive model. The mechanical characters of fiber, glassy phase and rubbery phase are embodied by the Generalized Hooke’s laws. Comparisons between model prediction and experimental results are presented too. Additionally, the elongation at break of carbon fiber which we used in this research as reinforcement is 1.8%, thus only small deformation was investigated in this study.

2. Materials and experiment

The matrix of the sample is a kind of epoxy based shape memory polymer which was developed by one of our research group member [41]. The reinforcement material is T700 Toray carbon fiber. A Perkin Elmer Dynamic Mechanical Analyzer (DMA-7) is used to perform a dynamic thermal scan at a frequency of 1 Hz in the temperature range of 25–250 °C. The size of the epoxy based shape memory polymer test specimen is approximately 5 × 3 × 1 mm. The purpose of the dynamic thermal scan is to determine the basic mechanical response, glass transition temperature and the elastic modulus of epoxy. According to DMA test, the trend of variation in storage modulus and tangent delta with the changing temperature is illustrated in Fig. 1. It is clearly observed that the glass transition temperature T_g of the SMP samples is 100 °C.

To verify the efficiency of the developed model, conventional uniaxial tension tests are carried out according to ASTM-D638 stands, using a Zwick/roell testing machine equipped with a thermal chamber. The SMPCs samples used for uniaxial tension tests is a kind of SMPs matrix composites, consist of a ‘stiff’ fiber reinforcement and a ‘softer’ SMPs matrix arranged together with one phase distributed as an array inside of the other phase. To eliminate the effect of thermal expansion, experiment data will only start to adopt once the temperature reaches the design temperature for about 10 min. The experiment data can be collected by using software linked to devices. Tests are running at a constant stretching speed of 1 mm/min. Fig. 2(A–C) presents the stress–strain response of samples with different fiber volume fraction at a low temperature (30 °C) corresponding to the glassy state, at a high

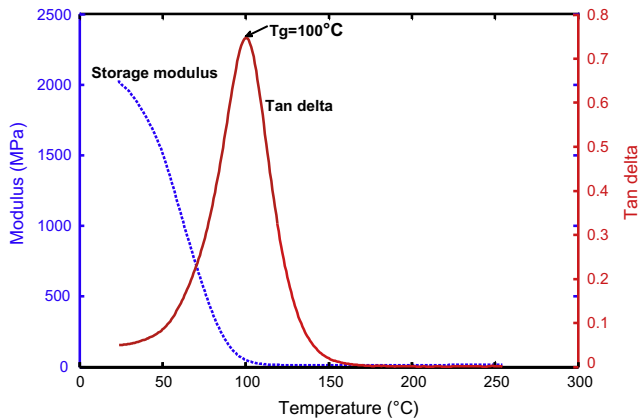


Fig. 1. The DMA test: storage modulus and tan delta of the shape memory polymer. (For interpretation of the references to color in this figure legend, the reader is referred to the web version of this article.)

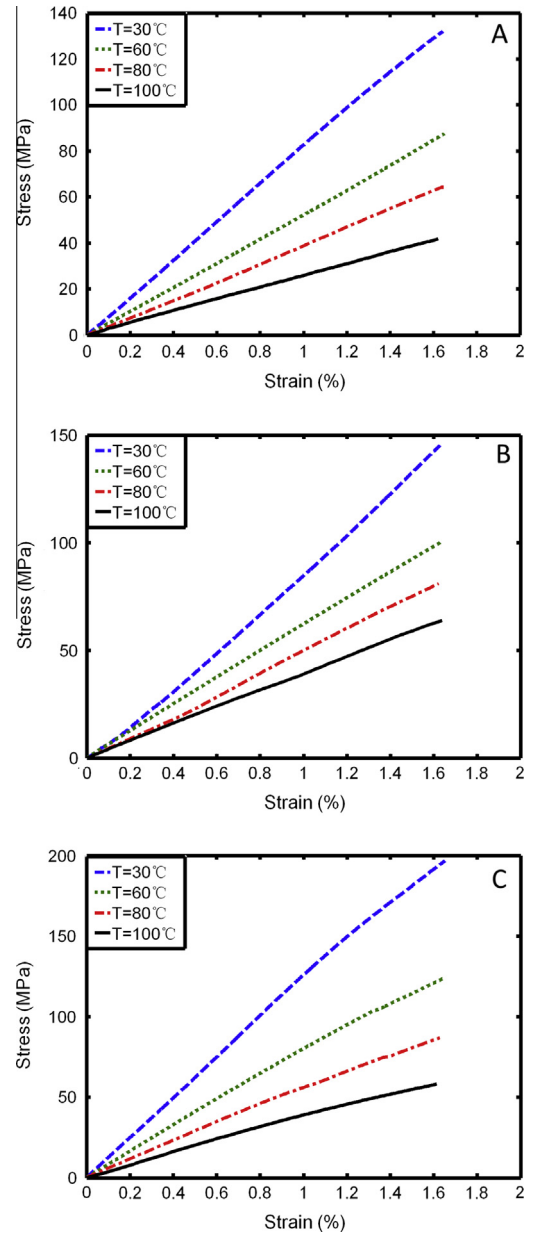


Fig. 2. Stress–strain diagram illustrating the thermo-mechanical behavior of shape memory polymer composite at different temperatures: (A) fiber content 7.5%, (B) fiber content 8.2%, (C) fiber content 11.5%. (For interpretation of the references to color in this figure legend, the reader is referred to the web version of this article.)

temperature (100 °C) corresponding to the rubbery state, and at an intermediate temperature (60 °C, 80 °C).

3. Constitutive model

3.1. Overall model description

In this study, SMPCs has been divided into shape memory polymer matrix and fiber reinforcement two segments. Based on the two phase theory of Liu, shape memory polymer matrix can be divided into glassy phase and rubbery phase two parts, which can be transformed to each other gradually with changed temperature [24]. In this 3-D model, the “frozen fraction” (glassy phase), the “active fraction” (rubbery phase) and the fiber fraction is respectively defined as:

$$\phi_g = \frac{V_{gla}}{V_{matrix}} = \frac{V_{gla}}{V_{gla} + V_{rub}}, \quad \phi_r = 1 - \phi_g \quad (1)$$

$$\psi_g = \frac{V_{gla}}{V}, \quad \psi_r = \frac{V_{rub}}{V}, \quad \psi_f = \frac{V_{fiber}}{V}, \quad \psi_m = \psi_g + \psi_r \quad (2)$$

$$V = V_{matrix} + V_{fiber} = V_{gla} + V_{rub} + V_{fiber}, \quad \psi_g + \psi_r + \psi_f = 1 \quad (3)$$

Here V , V_{gla} , V_{rub} , V_{fiber} denote the total volume of the SMPCs, volume of glassy phase, rubbery phase and, fiber reinforcement separately. And ψ_g denote the volume fraction of the glassy phase and ψ_r denote the volume fraction of rubbery phase, ψ_f denote the volume fraction of carbon fiber. V_{fiber} is invariable. The shape memory effect is caused by the transition of a crosslinking polymer from a state dominated by entropic energy (rubbery state) to a state dominated by internal energy (glassy state) as the temperature changes. By which, the glass transition during a thermo-mechanical cycle is reflected and the shape memory behavior can be captured, as schematically illustrated in Fig. 3.

Further, the total strain in SMPCs has been divided into five parts: glassy phase strain, rubbery phase strain, fiber strain, stored strain and thermal strain. Thus the strain can be expressed in Eq. (3) as:

$$\varepsilon_i = \varepsilon_i^f \psi_f + \varepsilon_i^g \psi_g + \varepsilon_i^r \psi_r + \varepsilon_T + \varepsilon_{gs}^n \quad (4)$$

where superscript g , r and f stands for glassy phase, rubbery phase and fiber separately, and ε_T represent thermal strain, ε_{gs}^n denote the strain stored and released during the cooling and heating process. Correspondently, the stress can be divided into five parts, which can be expressed in Eqs. (5)–(7) as:

$$\sigma_i = \sigma_i^T + \sigma_i^{rec} + \sigma_i^C \quad (5)$$

$$\sigma_i^C = \psi_f \sigma_i^f + \psi_g \sigma_i^g + \psi_r \sigma_i^r \quad (6)$$

$$\sigma_i^m = \phi_g \sigma_i^g + \phi_r \sigma_i^r \quad (7)$$

where superscript C and m denote composite and matrix separately. And σ_i^{rec} represent recovery stress.

3.2. Composite bridging model

A unidirectional fiber reinforced composite micro-mechanics model must follow the relationship below [39,40].

$$\sigma_i^C = \psi_f \sigma_i^f + \psi_m \sigma_i^m \quad (8)$$

$$\varepsilon_i^C = \psi_f \varepsilon_i^f + \psi_m \varepsilon_i^m \quad (9)$$

Here ψ_f is volume fraction of fiber, ψ_m is volume fraction of matrix and σ_j denote the external stress exert on SMPCs. And ε_i^m , ε_i^f , σ_i^m , σ_i^f denote the strain and stress of shape memory polymer matrix and fiber reinforcement separately. Additionally, the fiber has to satisfy its own constitutive relation when the strain within the extent of elasticity

$$\varepsilon_i^f = [S_{ij}^f] \sigma_j^f \quad (10)$$

Here $[S_{ij}^f]$ is the flexibility matrix of fiber reinforcement.

It is assumed that the surface of the matrix is in direct contact with the fiber and bond together. Until the composite has been damaged the interface will not be de-bonding, or relatively displacement. Suppose the composite undamaged, these two internal stresses, σ_i^m and σ_j^f , can be related by a non-singular matrix.

$$\sigma_i^m = [A_{ij}] \sigma_j^f \quad (11)$$

Here $[A_{ij}]$ is bridging matrix. Insert Eq. (11) into Eq. (8), internal stress in fiber and matrix can be derived as:

$$\sigma_i^f = (\psi_f [I] + \psi_m [A_{ij}])^{-1} \sigma_j = [B_{ij}] \sigma_j^C \quad (12)$$

$$\sigma_i^m = [A_{ij}] (\psi_f [I] + \psi_m [A_{ij}])^{-1} \sigma_j = [A_{ij}] [B_{ij}] \sigma_j^C \quad (13)$$

Here $[I]$ is identity matrix. $[B_{ij}]$ is an inverse matrix of $(\psi_f [I] + \psi_m [A_{ij}])$, and the explicit expression of $[B_{ij}]$ will be given in the later section. Substitute Eq. (12) into Eq. (10), the internal strain in fiber can be derived as following:

$$\varepsilon_i^f = [S_{ij}^f] \sigma_j^f = [S_{ij}^f] [B_{ij}] \sigma_j^C \quad (14)$$

Here $[S_{ij}^f]$ denotes the flexibility matrix of fiber, the explicit expression will be given later. Although a material with two phases is inhomogeneous, we assume that the corresponding stresses in glassy phase and rubbery phase are equal to the stress in matrix [24]:

$$\sigma_i^r = \sigma_i^g = \sigma_i^m \quad (15)$$

3.3. Strains in the matrix

When at a temperature well below SMPs' glass transition temperature, hardness of SMPs is very high. At this point, the deformation is correlated to the external force, once the force has been removed, the deformation will recover immediately. At this temperature, large-scale conformational changes are not possible but localized conformational motions are allowed. Thus it is appropriate to adopt the Generalized Hooke's law to describe the glassy phase mechanical characteristics.

$$\varepsilon_i^g = S_g : \sigma_i^g \quad (16)$$

Here S_g denote the flexibility matrix of glassy phase. When the temperature is well above the SMPs' glass transition temperature, the polymer is in rubbery state. The stiffness of rubbery phase can be as low as several MPa, while the rubbery elastic strain can be on the order of several hundred percent with appropriate cross-linking density. Thus it is necessary to adopt a nonlinear hyper-elastic constitution equation to describe the rubbery phase large deformation. Yet the non-linearity of rubbery elasticity can be ignored for small strains, we can also assume that the material behaves in a linear

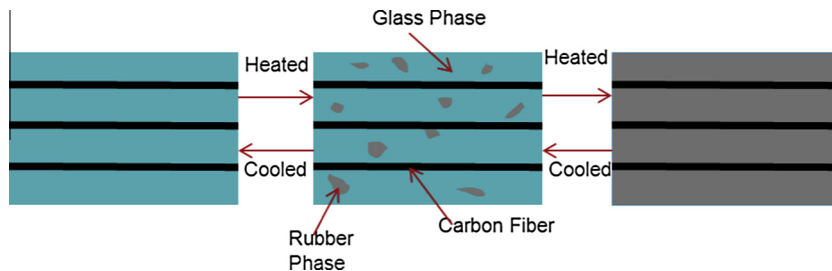


Fig. 3. Representative body element for SMPCs: transition between glassy state and rubbery state. (For interpretation of the references to color in this figure legend, the reader is referred to the web version of this article.)

elastic manner in the rubbery phases. Hence the strain of rubbery phase can also be related to the stress tensor through the Generalized Hooke's laws:

$$\varepsilon_i^r = S_r : \sigma_i^r \quad (17)$$

where S_r denote the flexibility matrix of rubbery phase.

3.4. Stored strain

The following specify stored strain ε_{gs} in the representative volume element dv . With a drop in temperature, a part of rubbery phase will translate into glassy phase gradually, at the same time the deformation previously in rubbery phase will be 'frozen' and stored. Here V_{froz} denotes the glassy phase volume which translates from rubbery phase. It is assumed that the elastic fiber reinforcement is evenly distributed in the SMPs matrix and the fiber in glassy phase and rubbery phase is evenly interlaced. During the process of strain storage, the fiber, which evenly distributed in rubbery phase, its deformation will fixed too as this part of rubbery phase translate into glassy phase. In SMPs application, firstly the composite is raised to above its glass transition temperature by external heater, it means that at this point the SMPs is completely in rubbery phase. Secondly a load has been applied on SMPs based structure, and then it will display elastic deformation. Maintain this deformation and cooled down the structure, the deformation will be fixed. So the total volume which has been frozen can be expressed as:

$$V_{froz} = V_g + \frac{V_g}{V_g + V_r} V_f \quad (18)$$

With the decreasing of temperature, a part of rubber phase (ΔV) translate into frozen phase. The growth of stored strain is $\Delta V \varepsilon_r$, and it can be expressed as following:

$$\varepsilon_{gs}^n = \frac{V_{froz} \varepsilon_{gs} + \Delta V \varepsilon_r}{V} \quad (19)$$

Here ε_r denote the strain in rubber phase. When rubber phase translates into frozen phase continuously, the stored strain changed continuously, and it can be expressed as:

$$\varepsilon_{gs}^n = \frac{V_{froz} \varepsilon_{gs} + \int_{V_{froz}} \varepsilon_r dV}{V} \quad (20)$$

Because $V_{froz} = V_g + \frac{V_g}{V_g + V_r} V_f = V \cdot \frac{\psi_g}{1 - \psi_f}$, thus the expression of ε_{gs}^n can be simplified as:

$$\varepsilon_{gs}^n = \frac{1}{1 - \psi_f} [\psi_{g1} \varepsilon_{gs} + (\psi_{g2} - \psi_{g1}) \varepsilon_r] \quad (21)$$

In the above equation, ψ_{g1} and ε_{gs} denote the volume fraction and strain of frozen phase at initial temperature, ψ_{g2} and ε_{gs}^n denote the volume fraction and strain of frozen phase at current temperature. It can be seen that the carbon fiber content has no impacts on stored strain.

With the increasing temperature, the stored strain will release gradually, include the part of frozen fiber. It will cause the reduction of stored strain in the whole body element. From macroscopic point of view, the deformation recovered. Therefore, the stored strain can be expressed as follow during the temperature increasing process.

$$\varepsilon_{gs}^n = \frac{\varepsilon_{gs} V_{froz}}{V} = \frac{\psi_g \varepsilon_{gs}}{1 - \psi_f} \quad (22)$$

When the temperature is increased from T_1 to T_2 , the stored strain which has been released is $(\varepsilon_{gs} - \varepsilon_{gs}^n)$. The recovery stress during the temperature increasing process can be extrapolated as:

$$\sigma_{rec} = \varepsilon_{gs} (\psi_{r1}(T_1) - \psi_{r2}(T_2)) (E_f \psi_f + E_r (1 - \psi_f)) \quad (23)$$

Here $\psi_{r1}(T_1)$ and $\psi_{r2}(T_2)$ denote the volume fraction of rubber phase at the initially temperature and current temperature separately.

3.5. Thermal strain

The total thermal strain ε_T of SMPs is constitutively defined as:

$$\varepsilon_T = \psi_r \varepsilon_T^r + \psi_g \varepsilon_T^g + \psi_f \varepsilon_T^f \quad (24)$$

Here we make an assumption that rubbery phase, glassy phase and carbon fiber are homogenous materials, and their thermal strains only related to thermal expansion coefficient separately, which means that the sole internal straining mechanism is thermal strain, thus the thermal strain can be simply defined as:

$$\varepsilon_T = \int_{T_0}^T \alpha dT \quad (25)$$

The thermal strain in glassy phase can be expressed as:

$$\varepsilon_T^g = \int_{T_0}^T \alpha_g dT \quad (26)$$

where α_g denote the thermal expansion coefficient of glassy phase. The thermal strain in rubbery phase can be expressed as the integral of thermal expansion coefficient of rubbery phase:

$$\varepsilon_T^r = \int_{T_0}^T \alpha_r dT \quad (27)$$

And the thermal strain in the fiber can be expressed as following:

$$\varepsilon_T^f = \int_{T_0}^T \alpha_f dT \quad (28)$$

Here α_r and α_f are the thermal expansion coefficient of rubbery phase and fiber separately. Thus the whole thermal strain can be expressed as following:

$$\varepsilon_T = \int_{T_0}^T [\psi_r(T) \alpha_r + \psi_g(T) \alpha_g + \psi_f(T) \alpha_f] dT \quad (29)$$

4. Results and discussion

4.1. Parameter identification

Based on the investigation of Liu YP, the young's modulus of shape memory polymer matrix can be related to ϕ_g as follows [24]:

$$E(T) = \frac{1}{\frac{\phi_g}{E_L} + \frac{1 - \phi_g}{3NkT}} \quad (30)$$

Here ϕ_g is the volume fraction of glassy phase, and N denote cross-link density. By analyzing the empirical data obtained in part 2, the relation between the elastic modulus and temperature is found to follow a power function. Thus the elastic modulus is obtained by fitting experimental data, and expressed as follows:

$$E(T) = le \left(\frac{b_1 - T}{c_1} \right)^2 + me \left(\frac{b_2 - T}{c_2} \right)^2 + ne \left(\frac{b_3 - T}{c_3} \right)^2 \quad (31)$$

The volume fraction of glassy phase can be derived from Eq. (30) as following:

$$\phi_g(T) = \frac{E_L(3NkT - E(T))}{E(T)(3NkT - E_L)} \quad (32)$$

The volume fraction of rubbery phase and glassy phase in SMP composite are expressed as following separately:

$$\psi_r(T) = (1 - \psi_f)(1 - \phi_g) \quad (33)$$

$$\psi_g(T) = (1 - \psi_f)\phi_g \quad (34)$$

The volume fraction of glassy phase, rubbery phase and fiber reinforcement is demonstrated in Fig. 4 separately. The fiber content remains invariable. At a temperature well above the SMPs glass transition temperature, volume fraction of rubbery phase is at its peak, $\psi_r(T_h) = 1 - \psi_f$. It can be seen from Fig. 4 that, the volume fraction of rubbery phase is reduced with the falling of the temperature, until reaching a low point at $\psi_r(T_l) = 0$. The changing trend of glassy phase volume fraction is opposite to that of rubbery phase.

Based on composite bridging model, the unidirectional composite flexibility matrix can be derived as:

$$[S_{ij}] = (\psi_f[S_{ij}^f] + \psi_m[S_{ij}^m][A_{ij}])(\psi_f[I] + \psi_m[A_{ij}])^{-1} \quad (35)$$

When the strain in the fiber and matrix is within the extent of elasticity, the flexibility matrix of both can be expressed as following:

$$[S_{ij}^f] = \begin{bmatrix} \frac{1}{E_{11}^f} & -\frac{\nu_{12}^f}{E_{11}^f} & 0 \\ -\frac{\nu_{12}^f}{E_{11}^f} & \frac{1}{E_{11}^f} & 0 \\ 0 & 0 & \frac{1}{G_{12}^f} \end{bmatrix}, \quad [S_{ij}^m] = \begin{bmatrix} \frac{1}{E_{11}^m} & -\frac{\nu_{12}^m}{E_{11}^m} & 0 \\ -\frac{\nu_{12}^m}{E_{11}^m} & \frac{1}{E_{11}^m} & 0 \\ 0 & 0 & \frac{1}{G_{12}^m} \end{bmatrix} \quad (36)$$

The above matrixes have been partitioned and substituted into Eq. (35), and the bridging matrix can be deduced in the following form:

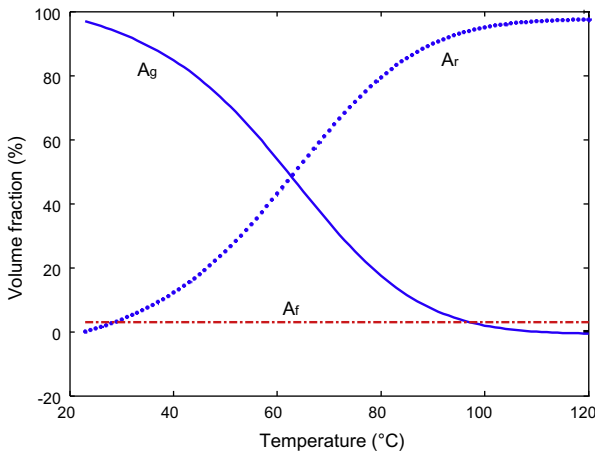


Fig. 4. Glassy phase/rubbery phase volume fraction, ψ_g , ψ_r , a function of temperature; ψ_f , a constant value. (For interpretation of the references to color in this figure legend, the reader is referred to the web version of this article.)

Table 1
Material parameters adopted from experiments and data fitting.

Material parameters	Values	Units	Description
E_g	2029.62	(MPa)	Young's modulus in the glass phase
E_r	14.11	(MPa)	Young's modulus in the rubber phase
E_f	230	(GPa)	Young's modulus of carbon fiber
l, m, n	0, 33.36, 0.0073	(-)	Parameter for storage modulus
b_1, b_2, b_3	1949, 7.738, 40.36	(-)	Parameter for storage modulus
c_1, c_2, c_3	856.6, 50.61, 28.6	(-)	Parameter for storage modulus
α_r	2.35×10^{-4}	(°C)	Rubber phase coefficient of thermal expansion
α_g	1.17×10^{-4}	(°C)	Glass phase coefficient of thermal expansion
α_f	-0.3×10^{-6}	(°C)	Carbon fiber coefficient of thermal expansion
T_l, T_g, T_h	27.8, 100, 120	(°C)	Temperature
α	0.4	(-)	Bridging parameter
β	0.32	(-)	Bridging parameter

$$[A_{ij}] = \begin{bmatrix} a_{11} & a_{12} & 0 \\ a_{21} & a_{22} & 0 \\ 0 & 0 & a_{33} \end{bmatrix} \quad (37)$$

The explicit expression of these parameters in Eq. (37) can be expressed as:

$$a_{11} = E^m/E_{11}^f \quad (38)$$

$$a_{12} = \frac{(S_{12}^f - S_{12}^m)(a_{22} - a_{11})}{S_{11}^m - S_{11}^f} \quad (39)$$

$$a_{22} = \beta + (1 - \beta)\frac{E^m}{E_{22}^f}, \quad 0 < \beta < 1 \quad (40)$$

$$a_{33} = \alpha + (1 - \alpha)\frac{G^m}{G_{12}^f}, \quad 0 < \alpha < 0 \quad (41)$$

$[B_{ij}]$, the converse matrix of bridging matrix $(\psi_f[I] + \psi_m[A_{ij}])$, can be expressed as:

$$[B_{ij}] = \begin{bmatrix} b_{11} & b_{12} & b_{13} \\ 0 & b_{22} & b_{23} \\ 0 & 0 & b_{33} \end{bmatrix} \quad (42)$$

The flowing are the specifically expressions of each parameter:

$$b_{11} = (\psi_f + \psi_m a_{11})^{-1} \quad (43)$$

$$b_{12} = -(\psi_m a_{12})/[(\psi_f + \psi_m a_{11})(\psi_f + \psi_m a_{22})] \quad (44)$$

$$b_{13} = [(\psi_m a_{12})(\psi_m a_{23}) - (\psi_f + \psi_m a_{22})(\psi_m a_{13})]/c \quad (45)$$

$$b_{22} = (\psi_f + \psi_m a_{22})^{-1} \quad (46)$$

$$b_{23} = -(\psi_m a_{23})(\psi_f + \psi_m a_{11})/c \quad (47)$$

$$b_{33} = (\psi_f + \psi_m a_{33})^{-1} \quad (48)$$

$$c = (\psi_f + \psi_m a_{11})(\psi_f + \psi_m a_{22})(\psi_f + \psi_m a_{33}) \quad (49)$$

Here, a part of material parameters in Table 1 come from DMA experimental result as illustrated in part 2, other parameters come from the coefficient of thermal expansion (CTE) experiments and data fit.

4.2. Model verification

Tension fatigue tests are carried out at different temperature to obtain the stress-strain curve of SMPCs samples with different fiber content, as mentioned before. To show the validity and accuracy of the model under different thermo-mechanical loadings conditions, the comparisons between the results of simulation and experiments have been made as show in Fig. 5(A–C). It is observed from Fig. 5 that there are deflections in varying degree between the experimental curve and the theoretical calculated curves. That mainly because the elastic modulus calculated by

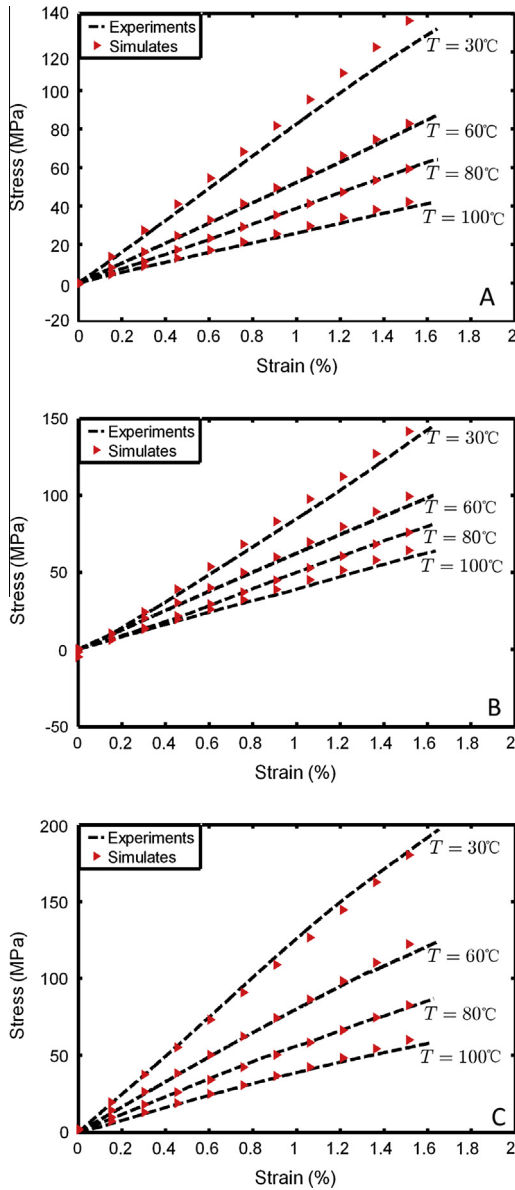


Fig. 5. Comparison between experiments and simulations: stress-strain diagram illustrating the thermo-mechanical behavior of shape memory polymer composite at different temperatures: (A) fiber content 7.5%, (B) fiber content 8.2%, (C) fiber content 11.5%. (For interpretation of the references to color in this figure legend, the reader is referred to the web version of this article.)

bridging model deviate from experiment results. And because errors are in an acceptable range, the correctness of the model has been verified generally.

It can be seen from Fig. 5 that the mathematical model captures the isothermal stress-strain behaviors of SMPCs at different temperatures and with different fiber contents. The results indicated that the stress σ which we need to sustain the same value of strain ϵ is increased with increase of fiber content ψ_f . This is because, based on the composite bridging model stress distribution principle $\sigma_i^f = [B_{ij}]\sigma_j$, most part of the stresses are supported by the carbon fiber. Because the elastic modulus of carbon fiber is as large as 230 GPa, even it undertaking most of the load, the increment of strain is very little. This result indicates that the fiber content brings great effect to mechanical properties of SMPCs, especially the strength of the material. Fig. 5 also illustrated that, compared with at temperature $T = 60^\circ\text{C}$ and $T = 80^\circ\text{C}$, the stress σ which we need to sustain the same value of strain ϵ is increased

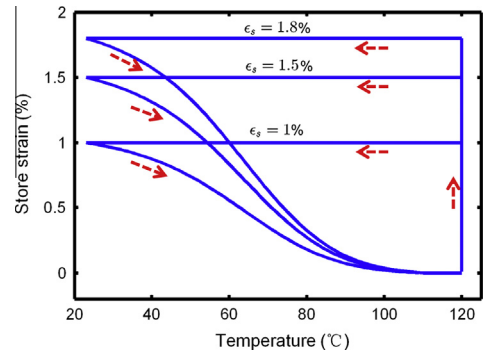


Fig. 6. Numerical simulations of store strain changing with decreasing of temperature. (For interpretation of the references to color in this figure legend, the reader is referred to the web version of this article.)

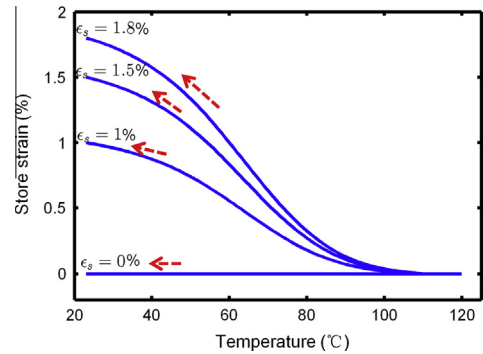


Fig. 7. Numerical simulations of store strain release with increasing of temperature. (For interpretation of the references to color in this figure legend, the reader is referred to the web version of this article.)

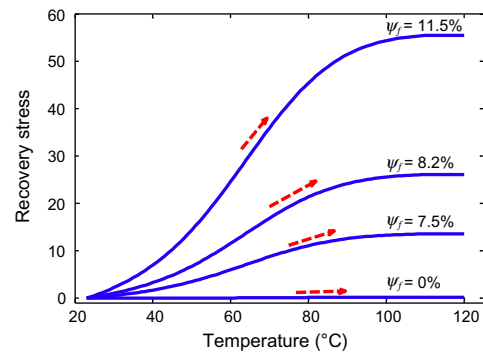


Fig. 8. Numerical simulations of stress-temperature behavior of the SMP composite from free shape recovery process: with different fiber content (0%, 7.5%, 8.2%, 11.5%). (For interpretation of the references to color in this figure legend, the reader is referred to the web version of this article.)

significantly at temperature $T = 30^\circ\text{C}$. That because with the increasing of temperature, the storage modulus of SMP decrease. Thus the modulus at $T = 30^\circ\text{C}$ is much higher than that at $T = 60^\circ\text{C}$, and for the time being the polymer translates from glass state into rubber state gradually. When at same load, the deformation of rubbery phase is much larger than glassy phase.

4.3. Recovery behaviors prediction

Using parameters in Table 1, the model is able to predict free recovery behaviors and the strain storage process. Fig. 6 shows the non-isothermal free recovery behaviors of SMP composite with different storage strain. Besides, the change trend of stored strain

with temperature is also predicted in Fig. 7. By contrasting the strain releasing in Fig. 6 and strain storage process in Fig. 7, it can be seen that, the strain storage process coincides with the non-isothermal free recovery behaviors, and these two curves almost overlap. In the application of SMPCs, such as SMPCs based space deployable structures, recovery force is an important index that evaluates mechanical performances of structures. The higher of the recovery force, the less of the hinge in need. Hence, it is vital to investigate how to improve the recovery force by changing fiber content. Fig. 8 shows the change trend of recovery stress under condition of constraint deformation of 2% and increasing temperature. It is observed that, with the rise of temperature, the recovery stress increase continuously as well. When the temperature is above SMPs glass transition temperature T_g , the recovery stress reaches the equilibrium point. Besides, the recovery stress is closely related to fiber content, and the recovery stress increase with fiber content.

5. Conclusion

The thermal mechanical behaviors of thermally induced unidirectional SMPCs had been investigated in this paper. Various experiments had been performed to fully characterize the complex thermal–mechanical response of unidirectional SMPCs and guide the development of the constitutive model. Composite bridging model had been employed to describe the relationship between fiber reinforcement and SMPs matrix by the constitutive model. Additionally, the concept that glassy phase and rubbery phase can exist in harmony and transform to each other as temperature change had been adopted.

It is assumed further that the stress in SMPs matrix is equal within both glassy phase and rubbery phase, and the Generalized Hooke's laws had been adopted to describe the elastic deformation of glassy phase and rubbery phase. The storage and releasing of strain had been further investigated during the cooling/heating process. Simulations of uniaxial tensile experiments under isothermal conditions agreed with the experimentally results. The thermal mechanically coupled constitutive model developed in this paper offers the potential for the development of a robust simulation-based capability for the design of devices made from unidirectional SMPCs for a variety of applications.

Acknowledgement

This work is supported by the National Natural Science Foundation of China (Grant Nos. 11225211, 11272106, and 11102052).

References

- [1] Lin JR, Chen LW. Study on shape-memory behavior of polyether based polyurethanes. I. Influence of the hard-segment content. *J Appl Polym Sci* 1998;69(15):63–74.
- [2] Lin JR, Chen LW. Study on shape-memory behavior of polyether based polyurethanes. II. Influence of the soft-segment molecular weight. *J Appl Polym Sci* 1998;69(15):75–86.
- [3] Jeong HM, Ahn BK, Cho SM, Kim BK. Water vapor permeability of shape memory polyurethane with amorphous reversible phase. *J Polym Sci: Part B: Polym Phys* 2000;38(30):9–17.
- [4] Lendlein A, Jiang H, Junger O, Langer R. Light induced shape memory polymers. *Nature* 2005;434(8):79–82.
- [5] Leng JS, Lu H, Liu Y, Huang W, Du S. Shape-memory polymers a class of novel smart materials. *MRS Bull* 2009;34(11):848–55.
- [6] Leng JS, Lan Xin, Liu YJ, Du SY. Shape-memory polymers and their composites: stimulus methods and applications. *Prog Mater Sci* 2011;56(7):1077–135.
- [7] Leng JS, Lv HB, Liu YJ, Du SY. Electroactivate shape memory polymer filled with nanocarbon particles and short carbon fibers. *Appl Phys Lett* 2007;91:144105.
- [8] Liu YJ, Lv HB, Lan X, Leng JS, Du SY. Review of electro-active shape-memory polymer composite. *Compos Sci Technol* 2009;69(13):2064–8.
- [9] Lv HB, Leng JS, Liu YJ, Du SY. Shape-memory polymer in response to solution. *Adv Eng Mater* 2008;10(6).
- [10] Leng JS, Lan X, Liu YJ, Du SY, Huang WM, Liu N, et al. Electrical conductivity of thermoresponsive shape-memory polymer with embedded microsized Ni powder chains. *Appl Phys Lett* 2008;92:014104.
- [11] Leng JS, Huang WM, Lan X, Liu YJ, Liu N, Phee SY, et al. Significantly reducing electrical resistivity by forming conductive Ni chains in a polyurethane shape-memory polymer/carbon-black composite. *Appl Phys Lett* 2008;92:204101.
- [12] Leng JS, Zhang Dawei, Liu Yanju, Yu Kai, Lan Xin. Study on the activation of styrene-based shape memory polymer by medium-infrared laser light. *Appl Phys Lett* 2010;96:111905.
- [13] Gall K, Mikulas M, Munshi NA, Beavers F, Tupper M. Carbon fiber reinforced shape memory polymer composites. *J Intell Mater Syst Struct* 2000;11(11):877–86.
- [14] Wei ZG, Sanstrom R. Shape memory materials and hybrid composites for smart systems: Part I. Shape-memory materials. *J Mater Sci* 1998;33(37):43–62.
- [15] Leng JS, Lv HB, Liu YJ, Du SY. Electro-activate shape memory polymer filled with nanocarbon particles and short carbon fibers. *Appl Phys Lett* 2007;91:144105.
- [16] Ta Ohki, Ni Q-Q, Ohsako N, Iwamoto M. Mechanical and shape memory behavior of composites with shape memory polymer. *Composites: Part A* 2004;35(9):65–73.
- [17] Gall K, Dunn ML, Liu Y, Finch D, Lake M, Munshi NA. Shape memory polymer nanocomposites. *Acta Mater* 2002;50(20):15–26.
- [18] Lu HB, Yu K, Sun SH, et al. Mechanical and shape-memory behavior of shape-memory polymer composites with hybrid fillers. *Polym Int* 2010;59(6):766–71.
- [19] Li G, Nettles D. Thermomechanical characterization of a shape memory polymer based self-repairing syntactic foam. *Polymer* 2010;51(3):755–62.
- [20] Li G, Xu W. Thermomechanical behavior of thermoset shape memory polymer programmed by cold-compression: testing and constitutive modeling. *J Mech Phys Solids* 2011;59(6):1231–50.
- [21] Tobushi H, Hayashi S. Properties and application of shape memory polymer polyurethane series. *Res Mach* 1994;46(6):646–52.
- [22] Lan X, Liu YJ, Lv HB, Wang XH, Leng JS, Du SY. Fiber reinforced shape-memory polymer composite and its application in a deployable hinge. *Smart Mater Struct* 2007;18(2):024002.
- [23] Zhang CS, Ni QQ. Bending behavior of shape memory polymer based laminates. *Compos Struct* 2007;78(2):153–61.
- [24] Liu Y, Gall K, Dunn M, Greenberg A, Diani J. Thermomechanics of shape memory polymers: uniaxial experiments and constitutive modeling. *Int J Plasticity* 2006;22(2):279–313.
- [25] Diani J, Liu Y, Gall K. Finite strain 3D thermoviscoelastic constitutive model for shape memory polymers. *Polym Eng Sci* 2006;46(4):486–92.
- [26] Chen YC, Lagoudas DC. A constitutive theory for shape memory polymers. Part I. Large deformations. *J Mech Phys Solids* 2008;56(5):1752–65.
- [27] Chen YC, Lagoudas DC. A constitutive theory for shape memory polymers. Part II. A linearized model for small deformations. *J Mech Phys Solids* 2008;56(5):1766–78.
- [28] Qi H, Nguyen T, Castro F, Yakacki C, Shandas R. Finite deformation thermo-mechanical behavior of thermally induced shape memory polymers. *J Mech Phys Solids* 2008;56(5):1730–51.
- [29] Kim J, Kang T, Yu W. Thermo-mechanical constitutive modeling of shape memory polyurethanes using a phenomenological approach. *Int J Plasticity* 2010;26(2):204–18.
- [30] Reese S. A micromechanically motivated material model for the thermoviscoelastic material behaviour of rubber-like polymers. *Int J Plasticity* 2003;19(7):909–40.
- [31] Xu W, Li G. Constitutive modeling of shape memory polymer based self-healing syntactic foam. *Int J Solids Struct* 2010;47(9):1306–16.
- [32] Baghani M, Naghdabadi R, Arghavani J, Sohrabpour S. A constitutive model for shape memory polymers with application to torsion of prismatic bars. *J Intell Mater Syst Struct* 2012;23(7):107–16.
- [33] Liu YP, Gall K, Dunn ML, Greenberg AR, Diani J. Thermomechanics of shape memory polymers: uniaxial experiments and constitutive modeling. *Int J Plasticity* 2006;22(2):279–313.
- [34] Barot G, Rao IJ. Constitutive modeling of the mechanics associated with crystallizable shape memory polymers. *Z Angew Math Phys* 2006;57(4):652–81.
- [35] Barot G, Rao IJ, Rajagopal KR. A thermodynamic framework for the modeling of crystallizable shape memory polymers. *Int J Eng Sci* 2008;46(4):325–51.
- [36] Tobushi H, Hara H, Yamada E, Hayashi S. Thermomechanical properties in a thin film of shape memory polymer of polyurethane series. *Smart Mater Struct* 1996;2716(5):483–91.
- [37] Nguyen TD, Qi HJ, Castro F, Long KN. A thermoviscoelastic model for amorphous shape memory polymers: incorporating structural and stress relaxation. *J Mech Phys Solids* 2008;56(9):2792–814.
- [38] Castro F, Westbrook K, Long K, Shandas R, Qi H. Effects of thermal rates on the thermomechanical behaviors of amorphous shape memory polymers. *Mech Time-Depend Mater* 2010;14(3):219–41.
- [39] Huang ZM. Simulation of the mechanical properties of fibrous composites by the bridging micromechanics model. *Composites Part A* 2001;32(2):143–72.
- [40] Huang ZM. Strength formulae of unidirectional composites including thermal residual stresses. *Mater Lett* 2000;43(1–2):36–42.
- [41] Leng Jinsong, Xuelian Wu, Liu Yanju. Effect of linear monomer on thermomechanical properties of epoxy shape memory polymers. *Smart Mater Struct* 2009;18(9):095031.